DESY 93-179
PSI-PR-93-23
WUB 93-39

The Leptonic Decay Constants of $\bar{Q}q$ Mesons and the Lattice Resolution[1]

C. Alexandrou[a 2], S. Güsken[b], F. Jegerlehner[c], K. Schilling[b], G. Siegert[b], R. Sommer[d]

[a] *Paul Scherrer Institut, CH-5232 Villigen PSI, Switzerland* and *Department of Natural Sciences, University of Cyprus, Nicosia, Cyprus*
[b] *Physics Department, University of Wuppertal, D-42097 Wuppertal, Germany*
[c] *Paul Scherrer Institut, CH-5232 Villigen PSI, Switzerland*
[d] *DESY, Theory Division, D-22603 Hamburg, Germany*

Abstract

We present a high statistics study of the leptonic decay constant f_P of heavy pseudoscalar mesons using propagating heavy Wilson quarks within the quenched approximation, on lattices covering sizes from about 0.7 fm to 2 fm. Varying β between 5.74 and 6.26 we observe a sizeable a dependence of f_P when one uses the quark field normalization that was suggested by Kronfeld and Mackenzie, compared with the weaker dependence observed for the standard relativistic norm. The two schemes come into agreement when one extrapolates to $a \to 0$. The extrapolations needed to reach the continuum quantity f_B introduce large errors and lead to the value $f_B = 0.18(5)$ GeV in the quenched approximation. This suggests that much more effort will be needed to obtain an accurate lattice prediction for f_B.

[1]work supported in part by DFG grant Schi 257/3-1.
[2]Present address: Department of Natural Sciences, University of Cyprus, Nicosia, Cyprus.

1. Introduction

The weak decays of D- and B-mesons will allow to extract the Cabibbo-Kobayashi-Maskawa matrix elements from the experimental data, once the hadronic interactions in the relevant weak matrix elements are determined from QCD. Lattice calculations in principle enable us to compute these QCD effects without model assumptions.

The simulation of heavy-light quark systems in lattice QCD requires lattice spacings a smaller than the inverse relevant masses. At present one reaches values $a^{-1} \sim 2$ to 4 GeV such that D-meson properties are amenable to lattice techniques.

The B-meson cannot be handled in such a direct way with lattice methods. The static approximation on the lattice [1] enables us to calculate the properties of pseudoscalar mesons in the limit of infinite quark mass, and it is very natural to estimate the B-meson matrix elements by interpolating between the D-mass range and the static point. The latter has been investigated by various groups [2, 3, 4, 5, 6, 7, 8], and it has been shown that (depending on the way one sets the scale) within the range $5.7 < \beta < 6.3$, the value of the leptonic decay constant f_{stat} changes significantly with the lattice resolution [4, 9]. Although the conventional *i.e. nonstatic* treatment of 'heavy' quarks (applied within — and slightly beyond — the charm region) has been pursued by a number of groups [10], the a dependence of f_P has not yet been systematically studied.

As actual lattice calculations with relativistic heavy quarks do not respect the inequality $am_q \ll 1$, lattice artifacts are an important issue. It has been suggested that lattice artifacts might be reduced by a modification of the relativistic normalization of states, $\sqrt{2\kappa}$, at order $O(am_q)$ [6, 11, 12, 13, 14]. In particular, Kronfeld and Mackenzie [13] have given arguments, that heavy quark fields in the Wilson formulation should be normalized by $\sqrt{1-3\kappa/4\kappa_c}$, which differs significantly from the naive normalization. This has been shown to yield a much smoother $1/M_P$ behaviour towards the static point at a fixed lattice spacing [6, 7].

The real check of improvement is to observe a flatter a-dependence of f_P at fixed m_q. In this paper we address this issue by presenting the results of a high statistics study of lattices at β= 5.74, 6.00 and 6.26 (with lattice extensions between 0.7 fm to 2 fm and inverse lattice spacings between 1.2 and 3.2 GeV). The results were obtained using standard Wilson fermions in the quenched approximation. Smearing techniques were needed to improve the saturation of the weak current correlators by the lowest lying states at large times.

The paper is organized as follows: In Section 2 we discuss some details of the calculation, in particular the smearing of operators applied to improve the signals at large time separations. We present a factorization test among local-local, local-smeared and smeared-smeared correlators to ensure ground state dominance. In Section 3 we briefly describe the Kronfeld-Mackenzie proposal to normalize heavy-light states. Our main results are contained in Section 4 where the a-dependence and finite size effects of the leptonic decay constant is presented and the implication of the Kronfeld-Mackenzie normalization

at finite values of a is discussed. After extrapolation to the continuum, we perform the interpolation between conventional results and the static point, to obtain the estimate for f_B. Summary and conclusions follow in Section 5.

2. Operators and Smearing

The starting point of this paper is our recent study of leptonic decay constants of heavy-light mesons in the static quark limit [4]. There, we optimized our trial wave functions with respect to maximal ground state dominance. In the following we will use the 'best' wave function, i.e. a 'gaussian type' wave function with parameters $n = 100$ and $\alpha = 4$, from ref. [4], where the reader will find more details about our simulation. The parameters of the lattices studied in this work are listed in table 1.

The pseudoscalar decay constant f_P is extracted from the lattice matrix element through the relation

$$< 0|\mathcal{M}^{loc}_{\gamma_4\gamma_5}|P >= Z_A^{-1}\sqrt{M_P/2}\, f_P\, a^{3/2} \quad . \tag{1}$$

Z_A is the axial current renormalisation constant, $\mathcal{M}^{loc}_{\gamma_4\gamma_5}$ is the fourth component of the local axial vector current, and $|P >$ denotes the pseudoscalar ground state. The precise normalization is further discussed in section 3. We define a generalized lattice current by

$$\mathcal{M}^J_\Gamma(\vec{x},t) = \bar{h}(\vec{x},t)\,\Gamma\, l^J(\vec{x},t) \tag{2}$$

where

$$l^J(\vec{x},t) = \sum_{\vec{y}} \Phi^J(\vec{x},\vec{y},\mathcal{U}(t))\, l(\vec{y},t) \tag{3}$$

is a smeared light (l) quark field obtained by applying the trial wave function Φ^J and $h(\vec{x},t)$ the local heavy (h) quark field.[3]

The aim is to extract the local matrix element by using wave functions optimized to yield early ground state dominance in the meson-meson correlator

$$C^{I,J}_\Gamma(t) = \sum_{\vec{x}} < \mathcal{M}^I_\Gamma(\vec{x},t)\,[\mathcal{M}^J_\Gamma(\vec{0},0)]^\dagger > \quad . \tag{4}$$

We consider four methods to extract the *local* matrix element $< 0|\mathcal{M}^{loc}_{\gamma_4\gamma_5}|P >$ from the local-smeared and smeared-smeared correlators:

(a) A three-parameter simultaneous fit to $C^{loc,J}_{\gamma_4\gamma_5}(t)$ and $C^{J,J}_{\gamma_4\gamma_5}(t)$ with equal mass in both correlators.

(b) Same as (a), but with correlators $C^{J,J}_{\gamma_5}(t)$ and $\sum_{\vec{x}} < \mathcal{M}^{loc}_{\gamma_4\gamma_5}(\vec{x},t)\,[\mathcal{M}^J_{\gamma_5}(\vec{0},0)]^\dagger >$.

[3] Since only smeared light quark fields are needed for the present investigation we suppress the source index for the heavy quark field which was used in ref. [4].

(c) A constrained fit to the local-smeared correlator $C^{loc,J}_{\gamma_4\gamma_5}(t)$, using the mass extracted from the smeared-smeared correlator, $C^{J,J}_{\gamma_4\gamma_5}(t)$.

(d) A fit to the ratio

$$R(t) = \frac{C^{loc,J}_{\gamma_4\gamma_5}(t)}{\sqrt{C^{J,J}_{\gamma_4\gamma_5}(t)}} \quad \stackrel{t \text{ large}}{\rightarrow} \quad < 0|\mathcal{M}^{loc}_{\gamma_4\gamma_5}|P > \; e^{-M_P t/2} \quad . \tag{5}$$

All fits (unless stated otherwise) have been carried out with the inverse covariance matrix but we have checked that the mean values are not significantly different from the ones resulting from a diagonal χ^2 fit. Ground state dominance has been monitored both by χ^2 and by the plateau in the local mass

$$\mu^{I,J}_\Gamma = \ln \frac{C^{I,J}_\Gamma(t)}{C^{I,J}_\Gamma(t-a)} \quad \text{in cases (a) – (c)} \tag{6}$$

or

$$\mu_R(t) = \ln \frac{R(t)}{R(t-a)} \quad \text{in case (d).} \tag{7}$$

In table 2, we show the results of the different methods for various heavy-light quark combinations. Methods (a) – (d) are seen to yield compatible results once ground state dominance is established by a low χ^2 value.

For the subsequent analysis we chose to apply method (d). The quality of the ground state dominance achieved is demonstrated in figure 1 which shows the local masses for β =5.74, 6.00 and 6.26 at a light quark mass of about $2m_s$. We list our results for f_P and M_P at several combinations of quark masses in table 3.

2.1 How good are local operators?

Having established the success of our smearing techniques we are in the position to examine the onset of ground state dominance in the case of purely local correlators. The ratio of smeared and local correlators[15]

$$r_\Gamma(t) = \frac{C^{J,J}_\Gamma(t) \;\; C^{loc,loc}_\Gamma(t)}{(C^{loc,J}_\Gamma(t))^2} \tag{8}$$

can be expressed in terms of completely local quantities for sufficiently large time separations t,

$$r^{as}_\Gamma(t) = \left(1 + \alpha^2_{loc} \, \frac{e^{-(m+\Delta)t} + e^{-(m+\Delta)(T-t)}}{e^{-mt} + e^{-m(T-t)}}\right), \tag{9}$$

if the correlators are dominated by two states with energies m and $m+\Delta$:

$$\begin{aligned} C^{I,J}_\Gamma &= A^0_I \, A^0_J (e^{-mt} + e^{-m(T-t)}) + A^1_I \, A^1_J (e^{-(m+\Delta)t} + e^{-(m+\Delta)(T-t)}) \\ A^n_I &= < 0|\mathcal{M}^I_{\gamma_4\gamma_5}|P, n > \end{aligned} \tag{10}$$

and as long as smearing has been operative in the sense that it has suppressed the excited state significantly:

$$\alpha_J \equiv A_J^1/A_J^0 \ll \alpha_{loc} \equiv A_{loc}^1/A_{loc}^0 \ . \tag{11}$$

The merits of this factorization test are the following:

- up to terms of order α_J^2 the ratio is purely dependent on the local parameters,
- the realm of ground state dominance can be clearly identified since the height of the plateau is known to be one,
- the ratio is dimensionless and has a continuum limit in the range where eq. 9 holds.

In order to determine the onset of ground state dominance in the purely local case we use the combined set of the present data and our previous local results [3, 16] as an input to eq. 8. We show the ratio $r_{\gamma_4\gamma_5}$ in figure 2 at $\beta = 6.26$ for fixed light quark mass ($m_l \simeq 2m_s$) and different heavy quark masses as a function of the time separation in units of GeV^{-1}. It appears that the plateau regime is reached only at about 5 GeV^{-1}. The local data alone seem to allow for an earlier plateau in the local mass. According to the present test, however, exploiting the local data under the assumption of ground state dominance at smaller time separations leads to an overestimation of f_P [16]. The pre-asymptotic behaviour according to eq. 9 is reflected by the data with a mass gap in the region of 600 MeV as illustrated by the dashed lines in figure 2.

At all values of the heavy quark mass that we investigated, the gap is consistent with ~ 600 MeV. The amplitude α_{loc} does, however, increase significantly when the mass of the heavy quark is increased. This entails that the *mass–dependence* of the decay constant is affected by fitting too early. On the basis of the present data, we estimate that this effect is of the order of the statistical errors for the $\beta = 6.4$ data of ref. [17] as well as for the $\beta = 6.26$ results of ref. [16].

In the above interpretation we rely on eq. 11. To some extent this equation is checked by the lattice spacing independence of r_Γ which results from eq. 11 (of course, as for any observable that has a continuum limit, the normal kind of a–effects should be there). In figure 3 we display r_Γ for different values of β. In agreement with eq. 11, we find that r_Γ is independent of β within the statistical errors.

3. Renormalization

Our quark fields are normalized according to the relativistic normalization (see ref. [4] for the form of the action). Due to the broken chiral symmetry in the Wilson formulation, the lattice axial vector current needs a finite renormalization [18]

$$A_\mu = Z_A \mathcal{M}^{loc}_{\gamma_\mu\gamma_5} \ . \tag{12}$$

As an intrinsic short distance quantity, Z_A can be calculated in perturbation theory, which at one-loop order gives [19]

$$Z_A = 1 - 0.1333\, g^2 \quad . \tag{13}$$

Since the next order term is so far unknown, it is not *a priori* clear which coupling constant g should be used to evaluate Z_A numerically. It is known that the bare coupling g_0 is not a good expansion parameter [20]. A recent analysis of a number of short distance dominated quantities by Lepage and Mackenzie [20] revealed that a mean field approach [21], which absorbs lattice tadpole contributions into effective quantities in the Wilson action, leads to a substantially better agreement between lattice Monte Carlo results and their perturbative expansions. We therefore use in the following the mean field improved coupling

$$\tilde{g}^2 = g_0^2/P \quad \text{with } P =< \frac{1}{3}\mathrm{TrP}_{\mu\nu} > , \tag{14}$$

as determined from the Monte Carlo simulation. In detail, also other forms of mean field improvements are being used [20, 6], but we note that they do not differ appreciably in numerical values and *we have to remember that the errors remain of order* $O(\tilde{g}^4)$ in any case.

Kronfeld and Mackenzie [13] have argued that for quark masses that are comparable to the inverse lattice spacing, an – at order $O(am_q)$ – different normalization of the axial vector current should have matrix elements with smaller lattice artifacts. For comparison, we use this nonrelativistic normalization

$$\tilde{A}_\mu = \tilde{Z}_A \sqrt{\frac{1}{2\kappa_l} - \frac{3}{8\kappa_c}} \sqrt{\frac{1}{2\kappa_h} - \frac{3}{8\kappa_c}} \mathcal{M}^{loc}_{\gamma_\mu\gamma_5} \ , \tag{15}$$

with l and h labelling the light and the heavy quark field. Here, κ_c denotes the critical value of the hopping parameter as determined from the vanishing of the pion mass. The renormalization constant $\tilde{Z}_A$ is given by [20]

$$\tilde{Z}_A = 1 - 0.0248\, \tilde{g}^2 \quad . \tag{16}$$

In the following section we will use both A_μ and $\tilde{A}_\mu$ for analyzing the data. The latter is denoted by 'KMc norm'.

4. Results

4.1 Finite a effects

In order to determine physical quantities from lattice calculations, it is crucial to perform the extrapolation $a \to 0$, within a chosen scale. In principle one would like to use f_π for this purpose, since then the $O(\tilde{g}^4)$ uncertainty in Z_A cancels. At present, the statistical errors of f_π in our simulation are however too large to pursue this approach. Therefore we will use the string tension, which has small statistical errors, during the extrapolation and convert the result finally into the most 'natural' scale, f_π. As stated in the introduction,

the supposed improvement of the normalization (eq. 15) should manifest itself in a smaller slope of $f_P(a)$ as a goes to zero [13]. The question is whether this is actually the case in the available range of β. In order to check this we have computed f_P both with the naive (standard relativistic) and the KMc norms at several pseudoscalar masses. The data from table 3 are extrapolated in the standard manner to the chiral limit (see ref. [4]) and are compiled in table 4. We have determined the a-dependence at fixed values of M_P within the range 1.1 GeV $\leq M_P \leq$ 2.3 GeV. In figure 4 we show the situation with relativistic norm and with the KMc norm. Note, that we had to interpolate between the computed M_P values in order to tune for fixed physical M_P as β is varied. The interpolation introduces only a minor uncertainty since the dependence of f_P on M_P is very weak. It was estimated by comparing two–point and three–point interpolations and added to the statistical errors.

It can be seen that the KMc norm has a sizeable impact on f_P at present values of the lattice spacing. Contrary to the expectations, however, $f_P(a)$ is turned from a very weakly decreasing into a strongly decreasing function. As we increase M_P the effect becomes more pronounced. Nevertheless the extrapolated values at $a = 0$ coincide. We have used a linear extrapolation and omitted those points where the effect of the KMc factor amounts to more than a 60 % change. The linear extrapolation functions have been followed back to the omitted points as dashed lines. These demonstrate that the extrapolation is stable, namely, within the statistical errors one would obtain the same result at $a = 0$ if all points were included in the extrapolation. Note that according to perturbative arguments, the leading lattice spacing dependence should be linear in a, *if* the $O(\tilde{g}^4)$ terms are numerically small. We come back to that point in section 4.3.

In figure 5 we display the effects of the KMc factor onto the quantity

$$\hat{f}_P = f_P \sqrt{M_P} \left(\frac{\alpha_s(M_P)}{\alpha_s(M_B)} \right)^{6/33} \quad . \tag{17}$$

The first impression is that at *fixed* and *finite* values of a the data in KMc norm interpolate smoothly between the D region and the static point and this has been interpreted as improvement [6, 7]. Given the conclusion from figure 4 the improvement does not survive the limit $a \to 0$, however. This is visualized in figure 5 by the error band which refers to the results of the above continuum extrapolation. Note also, that the poor scaling behavior of f_P in the KMc norm is already visible in figure 5.18 of ref. [6].

4.2 Finite size effects

The data we discussed above was obtained on lattices with periodicity in space L of magnitude $L\sqrt{\sigma} \sim 3$. Here we intend to consolidate our results with respect to possible finite size effects. For that purpose we have plotted in figure 6 f_P as a function of L for three pseudoscalars with fixed light quark mass of about $2m_s$ at $\beta = 5.74$. As expected finite size effects decrease with increasing heavy quark mass.

In the range $L\sqrt{\sigma} \geq 3$ we find no significant finite volume effects with a precision of the

order of $\sim 2\%$. Decreasing the light quark mass down to m_s we compare the $8^3 \times 24$ and $12^3 \times 24$ lattices at $\beta = 5.74$, c.f. table 3. There appears to be a small volume effect of maximally $3\% \pm 2\%$. This is, however, statistically not significant. So we have kept the volume fixed at $L\sqrt{\sigma} \sim 3$ throughout our final analysis, but estimate from the above analysis, that there may be a $\sim 5\%$ error involved with this.

4.3 Conversion to scale f_π

The most 'natural' scale for f_P is f_π, since the uncertainty due to the renormalization constant Z_A cancels out in this case and one may also hope, that the ratio f_P/f_π is not affected strongly by the quenched approximation. Lattice measurements of f_π are generally accompanied by large statistical errors and therefore we have decided to convert our results to this scale only after having performed the $a \to 0$ extrapolation of f_P. To achieve this we have decoupled the extrapolations according to

$$\frac{f_P}{f_\pi}(a \to 0) = \frac{f_P/\sqrt{\sigma}(a \to 0)}{f_\pi/\sqrt{\sigma}(a \to 0)} \quad . \tag{18}$$

To obtain the denominator of eq. 18 we used both our own data and the results of other lattice groups [6, 8, 22, 23] (all data has been changed to the relativistic normalization). The compilation of the data is shown in figure 7. Since the a dependence of $f_\pi/\sqrt{\sigma}$ is obviously weak, a linear extrapolation to $a = 0$ is well justified and leads to :

$$\frac{f_\pi}{\sqrt{\sigma}}(a = 0) = 0.269(12) \quad . \tag{19}$$

In addition to the quoted statistical error, this quantity has an uncertainty due to the missing $O(\tilde{g}^4)$ terms in Z_A. This should, however, largely cancel out when we take the ratio eq. 18.

4.4 Heavy mass extrapolation

In figure 8 we display our final results[4] at $a = 0$ in the form $\hat{f}_P(1/M_P)$, together with our static value from ref. [4]. As described in the previous section the scale has finally been converted to $f_\pi = 132$MeV. The new data appears to depend only weakly on M_P. Note however, that the data points carry error bars of order 25% and therefore do not exclude a stronger variation in M_P. This is due to the extrapolations to the chiral and continuum limits.

Given this situation we draw an error band that links the conventional results with the static point. The M_P dependence of the error band was chosen according to the ansatz

$$\hat{f}_P = c_0 + \frac{c_1}{M_P} + \frac{c_2}{M_P^2} \quad . \tag{20}$$

[4]To be specific the extrapolation has been performed on the data using the relativistic norm since it involves smaller statistical errors than using the KMc norm.

At the location of the B meson the error band corresponds to

$$f_B = 0.18(5)\text{GeV} \qquad . \tag{21}$$

It is evident from figure 8 that this value is strongly affected by the size and uncertainty of f_{stat}. From the direct continuum extrapolation at the mass of the D, we quote

$$f_D = 0.17(3)\text{GeV} \qquad . \tag{22}$$

At a given M_P one can extrapolate to $a \to 0$ the ratio f_{P_s}/f_P. In the ratio scale ambiguities drop out and additional systematic errors e.g. due to quenching may be reduced. We find that the heavy mass dependence of the ratio is very weak and can be taken as constant in the mass range between the charm and the B mesons. In the continuum limit we obtain $f_{P_s}/f_P = 1.09(2)$ at $L\sqrt{\sigma} \sim 3$, where the statistical error is quite small. We therefore have to remember the finite size uncertainty and finally quote

$$f_{P_s}/f_P = 1.09(2)(5).$$

5. Summary and conclusions

We have carried out a high statistics analysis of the pseudoscalar decay constant. In the case of purely local operators, the ground state signal is attained only at time separations larger than 5 GeV^{-1}. For this reason smearing techniques should also be applied in the nonstatic situation.

We observe little volume dependence of f_P as long as $L\sqrt{\sigma} \geq 3$. For $5.74 \leq \beta \leq 6.26$, we discover a marked variation with a, if the KMc normalization is used, while the relativistic normalization results in f_P-values that are rather insensitive to our variation of a. This implies that KMc does not yet lead to improvement in the sense that finite a results are shifted towards their continuum limit.

In this context, we emphasize that it is misleading to look only at the M_P dependence of f_P at one value of β. One rather has to work at different β values and to extrapolate to the continuum. Proceeding in this manner we find that the difference originating from the two normalizations vanishes, as it should.

We consider the present investigation as exploratory in spite of the statistics of about 100 independent configurations on the largest lattice. The estimates of f_B and f_D (see eqs. 21,22) still carry rather large errors originating from the unavoidable extrapolation in a. Study of the a dependence is also necessary when an improved action is used. The extrapolation errors can be greatly reduced with the power of available parallel supercomputers, by increasing the number of points in a with very high statistics.

As we have mentioned, it would also be desirable to perform the whole continuum extrapolation on the ratio f_P/f_π in order to be completely free of the uncertainties in Z_A.

It appears, however, that better ways of computing f_π need to be found before this is feasible.

Along the same lines, a study of the finite a effects of B_B is necessary, since it has been clearly demonstrated for the case of B_K that a effects do not necessarily cancel out for these observables [24].

Acknowledgements. The calculations were carried out on the NEC-SX3 at the Supercomputing Center in Manno, Switzerland and on the CRAY-Y-MP of the HLRZ in Jülich, Germany. We thank both institutions and their staff for their generous support.

References

[1] E. Eichten, in *"Field Theory on the Lattice"*, Nucl. Phys. B (Proc.Suppl.) 4 (1988) 147.

[2] C.R. Allton et al., Nucl. Phys. B349(1991)598.

[3] C. Alexandrou, S. Güsken, F. Jegerlehner, K. Schilling and R. Sommer, Phys. Lett. B256 (1991) 60.

[4] C. Alexandrou, S. Güsken, F. Jegerlehner, K. Schilling, and R. Sommer, PSI preprint, PSI-92-27, 1992, Nucl. Phys B, in press.

[5] A. Duncan, E. Eichten, A. X. El-Khadra, J. M. Flinn, B. R. Hill and H. Thacker, Nucl. Phys. B (Proc. Suppl.) 30(1993)433.

[6] C. Bernard, J. Labrenz, and A. Soni, preprint UW/PT-93-06, Wash. U HEP/93-30, BNL-49068, 1993

[7] UKQCD Collaboration, *Quenched Heavy-Light Decay Constants*, Edinburgh Preprint 93/526.

[8] The APE Collaboration, *A High Statistics Lattice Calculation in the Static Limit on APE*, Rome preprint 93/928.

[9] E. Eichten et al., Talk given at the *Lattice'93* conference in Dallas, to be published in Nucl. Phys. B (Proc. Suppl.).

[10] see refs. [6, 7, 16, 17] and references therein.

[11] S. Güsken, U. Löw, K.-H. Mütter, A. Patel, K. Schilling, and R. Sommer, Phys. Lett. B227: 266, 1989.

[12] C. Bernard, J. Labrenz and A. Soni, Nucl. Phys. B(Proc. Suppl.) 30 (1993) 465.

[13] G.P. Lepage, Nucl. Phys. B (Proc.Suppl.) 26 (1992) 45;
A.S. Kronfeld, Nucl. Phys. B (Proc. Suppl.) 30 (1993) 445;
P.B. Mackenzie, Nucl. Phys. B (Proc. Suppl.) 30 (1993) 35.

[14] G.P. Lepage and B.A. Thacker, in *Field Theory on the Lattice*, Nucl. Phys. B (Proc. Suppl.) 4 (1988) 199.

[15] E. Eichten, G. Hockney and H.B. Thacker, Nucl. Phys. B (Proc. Suppl.) 20 (1991) 500.

[16] C. Alexandrou, S. Güsken, F. Jegerlehner, K. Schilling, and R. Sommer, Nucl. Phys. B374 (1992) 263.

[17] A. Abada, C.R. Allton, P. Boucaud, D.B. Carpenter, M. Crisafulli, J. Galand, S. Güsken, G. Martinelli, O. Pene , C.T. Sachrajda, R. Sarno, K. Schilling and R. Sommer, Nucl. Phys. B376 (1992) 172.

[18] L. H. Karsten and J. Smit, Nucl.Phys. B183 (1981) 103.

[19] G. Martinelli and Y.-C. Zhang, Phys. Lett. 123B (1983) 433;
R. Groot, J. Hoek, and J. Smit, Nuc. Phys. B237 (1984) 111;
and references therein.

[20] G.P. Lepage and P.B. Mackenzie, Nucl. Phys. B(Proc. Suppl.) 20 (1991) 173 and Phys. Rev. D48(1993)2250.

[21] G. Parisi, in *"High–Energy Physics —1980"*, XX. Int. Conf., Madison (1980), ed. L. Durand and L.G. Pondrom (American Institute of Physics, New York, 1981).

[22] UKQCD Collaboration, *The Light Hadron Spectrum and Decay Constants in Quenched Lattice QCD*, Edinburgh Preprint 93/524.

[23] F. Butler, H. Chen, J. Sexton, A. Vaccarino and D. Weingarten, Phys. Rev. Lett. 70 (1993) 2849; D. Weingarten, private communication.

[24] S. Sharpe, Nucl. Phys. B (Proc.Suppl.) 26 (1992) 197;
N. Ishizuka, M. Fukugita, H. Mino, M. Okawa, Y. Shizawa and A. Ukawa, Nucl. Phys. B (Proc. Suppl.) 30 (1993) 415.

[25] G.S. Bali and K. Schilling, Phys. Rev. D46 (1992) 2636;
Phys. Rev. D47 (1993) 661.

Tables

Table 1:

Pseudoscalar decay constant and mass in lattice units as a function of $t_{\rm min}$, the smallest time separation used in the fit. Smearing is used for the light quark propagator. The results correspond to a light quark mass of about twice the strange quark mass (or $M(l,l)^2/\sigma \sim 4$). χ^2 denotes χ^2/d.o.f..

$\beta = 5.74 \quad \kappa_1 = 0.1560 \quad \kappa_2 = 0.1250$

$4^3 \times 24 \quad 404$ conf.

$t_{\rm min}$	af/Z_A	aM	χ^2
3	0.1954(39)	1.334(13)	uncorr.

$6^3 \times 24 \quad 131$ conf.

$t_{\rm min}$	af/Z_A	aM	χ^2
3	0.2159(18)	1.346(5)	uncorr.

$8^3 \times 24 \quad 175$ conf.

$t_{\rm min}$	af/Z_A	aM	χ^2
2	0.2270(19)	1.360(7)	3.1
3	0.2250(19)	1.359(6)	3.1
4	0.2222(22)	1.356(7)	2.5
5	0.2207(28)	1.355(5)	2.7
6	0.2169(35)	1.350(4)	2.6
7	0.2157(38)	1.350(6)	2.5
8	0.2209(43)	1.353(8)	2.3

$10^3 \times 24 \quad 213$ conf.

$t_{\rm min}$	af/Z_A	aM	χ^2
2	0.2257(9)	1.353(4)	2.9
3	0.2235(4)	1.353(5)	2.3
4	0.2206(16)	1.351(4)	1.5
5	0.2193(18)	1.350(3)	1.4
6	0.2166(18)	1.347(4)	0.4
7	0.2161(22)	1.347(5)	0.4
8	0.2148(32)	1.346(3)	0.3

$12^3 \times 24 \quad 113$ conf.

$t_{\rm min}$	af/Z_A	aM	χ^2
2	0.2212(4)	1.356(12)	1.0
3	0.2208(23)	1.355(3)	1.3
4	0.2181(20)	1.353(9)	0.6
5	0.2175(30)	1.353(3)	0.6
6	0.2172(28)	1.353(6)	0.8
7	0.2157(30)	1.351(7)	0.7
8	0.2153(36)	1.351(4)	1.0

$\beta = 6.00 \quad \kappa_1 = 0.1525 \quad \kappa_2 = 0.1250$

$12^3 \times 36 \quad 204$ conf.

$t_{\rm min}$	af/Z_A	aM	χ^2
3	0.1280(14)	1.080(2)	2.0
4	0.1277(14)	1.079(2)	2.0
5	0.1260(15)	1.078(3)	1.0
6	0.1266(15)	1.078(3)	1.1
7	0.1273(19)	1.079(3)	1.1
9	0.1270(19)	1.079(4)	1.4

$18^3 \times 36 \quad 9$ conf.

$t_{\rm min}$	af/Z_A	aM	χ^2
6	0.1281(54)	1.084(7)	uncorr.
7	0.1264(57)	1.082(7)	uncorr.
9	0.1208(76)	1.075(11)	uncorr.

$\beta = 6.26 \quad \kappa_1 = 0.1492 \quad \kappa_2 = 0.1200$

$12^3 \times 48 \quad 103$ conf.

$t_{\rm min}$	af/Z_A	aM	χ^2
4	0.0859(23)	1.040(5)	1.8
6	0.0845(34)	1.039(8)	2.0
8	0.0834(30)	1.039(6)	1.6
10	0.0853(46)	1.039(7)	1.2
12	0.0831(47)	1.035(7)	1.2
14	0.0808(48)	1.031(9)	1.2
16	0.0823(55)	1.033(8)	1.5

$18^3 \times 48 \quad 76$ conf.

$t_{\rm min}$	af/Z_A	aM	χ^2
4	0.0833(21)	1.039(7)	2.9
6	0.0813(21)	1.034(6)	2.0
8	0.0811(27)	1.034(5)	2.3
10	0.0784(29)	1.030(5)	1.3
12	0.0777(29)	1.029(5)	1.5
14	0.0805(39)	1.033(6)	1.5
16	0.0783(44)	1.030(7)	1.7

Table 2:

af/Z_A calculated with different methods as described in the text:
(a) simultaneous fit to $C^{J,J}_{\gamma_4\gamma_5}$ and $C^{loc,J}_{\gamma_4\gamma_5}$,
(b) simultaneous fit to $C^{J,J}_{\gamma_5}$ and $\sum_{\vec{x}} < M^{loc}_{\gamma_4\gamma_5}(\vec{x},t)[M^J_{\gamma_5}(\vec{0},0)]^\dagger >$,
(c) determine $a\,m_P$ by fit to $C^{J,J}_{\gamma_4\gamma_5}$ and use this as constraint in the fit to $C^{loc,J}_{\gamma_4\gamma_5}$,
(d) ratio method.
We show the results for the lattices used to obtain our final results. χ^2 actually denotes χ^2/d.o.f..

$$\beta = 5.74 \quad N_S^3 \times N_T = 8^3 \times 24 \quad \kappa_1 = 0.1560 \quad \kappa_2 = 0.1250$$

$t_{\min}$	(a)	χ^2	(b)	χ^2	(c)	χ^2	(d)	χ^2
2	0.2274(14)	2.8	0.2372(26)	8.8	0.2314(17)	6.8	0.2270(19)	3.1
3	0.2256(20)	2.6	0.2313(28)	6.9	0.2280(23)	3.0	0.2250(19)	3.1
4	0.2224(24)	2.1	0.2250(28)	4.1	0.2238(28)	2.2	0.2222(22)	2.5
5	0.2203(27)	1.9	0.2216(29)	3.4	0.2196(30)	1.6	0.2207(28)	2.7
6	0.2159(35)	1.7	0.2158(31)	1.4	0.2169(33)	2.0	0.2169(35)	2.6
7	0.2145(41)	2.0	0.2142(35)	1.4	0.2154(36)	2.6	0.2157(38)	2.5
8	0.2181(44)	1.7	0.2130(38)	1.8	0.2144(38)	1.3	0.2209(43)	2.3

$$\beta = 6.00 \quad N_S^3 \times N_T = 12^3 \times 36 \quad \kappa_1 = 0.1525 \quad \kappa_2 = 0.1250$$

$t_{\min}$	(a)	χ^2	(b)	χ^2	(c)	χ^2	(d)	χ^2
3	0.1267(14)	1.8	0.1333(14)	4.9	0.1309(16)	1.8	0.1280(17)	2.0
4	0.1266(10)	1.9	0.1318(15)	3.5	0.1303(16)	1.8	0.1277(14)	2.0
5	0.1251(14)	1.2	0.1307(15)	1.7	0.1268(20)	1.4	0.1260(15)	1.0
6	0.1257(17)	1.1	0.1296(18)	1.7	0.1281(16)	1.3	0.1266(15)	1.1
7	0.1262(22)	1.2	0.1282(20)	1.5	0.1286(20)	1.5	0.1273(19)	1.1
9	0.1248(20)	1.3	0.1257(23)	1.1	0.1257(26)	1.8	0.1270(19)	1.4
11	0.1236(26)	1.4	0.1243(23)	1.1	0.1231(30)	2.0	0.1258(24)	1.7

$$\beta = 6.26 \quad N_S^3 \times N_T = 18^3 \times 48 \quad \kappa_1 = 0.1492 \quad \kappa_2 = 0.1200$$

$t_{\min}$	(a)	χ^2	(b)	χ^2	(c)	χ^2	(d)	χ^2
4	0.0819(30)	2.5	0.0842(42)	3.3	0.0821(36)	2.2	0.0833(21)	2.9
6	0.0809(33)	2.6	0.0825(39)	2.7	0.0810(36)	2.3	0.0813(21)	2.0
8	0.0799(30)	2.6	0.0808(32)	2.8	0.0811(37)	2.4	0.0811(27)	2.3
10	0.0770(25)	1.6	0.0782(22)	1.3	0.0777(33)	1.4	0.0784(29)	1.3
12	0.0775(30)	1.6	0.0783(24)	1.2	0.0782(38)	1.7	0.0777(29)	1.5
14	0.0800(36)	1.5	0.0795(29)	1.1	0.0800(34)	1.8	0.0805(39)	1.5
16	0.0789(35)	1.5	0.0793(29)	1.2	0.0782(41)	1.7	0.0783(44)	1.7

Table 3:

Pseudoscalar decay constant and mass in lattice units. The data has been used in the detailed analysis to extract f_B and f_D, with the exception of the results at $\beta = 5.74$, $12^3 \times 24$. Smearing has been applied to the light quark propagator. κ_1 corresponds to the light quark. χ^2 actually denotes χ^2/d.o.f..

$\beta = 5.74 \quad N_S^3 \times N_T = 8^3 \times 24$

κ_1	κ_2	fit range	$a\,M$	$a\,f/Z_A$	χ^2
0.156	0.09	5–12	1.999(4)	0.1905(33)	1.0
	0.125	4–12	1.344(4)	0.2206(24)	2.8
	0.140	4–12	1.065(4)	0.2231(31)	3.0
	0.150	4–12	0.870(4)	0.2164(41)	2.4
	0.156	4–12	0.748(5)	0.2008(57)	2.4
0.162	0.09	5–12	1.924(8)	0.1750(40)	1.0
	0.125	4–12	1.261(2)	0.2022(23)	1.8
	0.140	4–12	0.969(5)	0.2037(33)	2.1
	0.150	4–12	0.761(4)	0.1972(48)	2.0
	0.162	5–12	0.474(8)	0.1608(58)	1.1
0.1635	0.09	5–12	1.904(10)	0.1697(43)	0.8
	0.125	4–12	1.242(7)	0.1973(24)	2.0
	0.140	4–12	0.948(5)	0.1997(30)	1.1
	0.150	4–12	0.734(4)	0.1917(44)	1.3
	0.1635	5–12	0.392(12)	0.1479(64)	1.1

$\beta = 5.74 \quad N_S^3 \times N_T = 12^3 \times 24$

κ_1	κ_2	fit range	$a\,M$	$a\,f/Z_A$	χ^2
0.156	0.09	5–12	2.001(6)	0.1872(24)	0.6
	0.125	4–12	1.354(5)	0.2179(24)	0.8
	0.140	4–12	1.073(7)	0.2207(12)	1.1
	0.150	4–12	0.878(5)	0.2133(23)	1.1
	0.156	4–12	0.755(5)	0.1959(24)	0.8
0.162	0.09	5–12	1.927(17)	0.1689(40)	0.8
	0.125	4–12	1.267(7)	0.1974(29)	0.6
	0.140	4–12	0.976(9)	0.2001(24)	1.0
	0.150	4–12	0.768(4)	0.1929(22)	1.1
	0.162	5–12	0.481(2)	0.1628(30)	0.8
0.1635	0.09	5–12	1.911(15)	0.1631(47)	0.7
	0.125	4–12	1.246(5)	0.1914(27)	0.5
	0.140	4–12	0.953(8)	0.1935(23)	0.9
	0.150	4–12	0.740(2)	0.1864(30)	1.1
	0.1635	5–12	0.395(4)	0.1523(35)	0.9

$\beta = 6.00 \quad N_S^3 \times N_T = 12^3 \times 36$

κ_1	κ_2	fit range	$a\,M$	$a\,f/Z_A$	χ^2
0.1525	0.10	5–13	1.574(7)	0.1060(15)	0.7
	0.115	5–13	1.279(3)	0.1186(14)	0.6
	0.125	5–18	1.077(2)	0.1260(15)	1.0
	0.135	5–18	0.870(3)	0.1349(13)	0.6
	0.145	7–18	0.649(1)	0.1301(23)	0.7
	0.1525	4–11	0.452(2)	0.1090(15)	0.6
0.1540	0.10	5–13	1.546(8)	0.1003(15)	0.7
	0.115	5–13	1.252(5)	0.1123(15)	0.6
	0.125	5–18	1.050(2)	0.1190(13)	1.0
	0.135	5–18	0.840(4)	0.1243(14)	0.6
	0.145	5–18	0.617(1)	0.1211(18)	0.9
	0.154	4–11	0.368(3)	0.0980(16)	0.7
0.1558	0.10	5–13	1.521(8)	0.0925(17)	1.1
	0.115	5–13	1.221(5)	0.1036(16)	1.1
	0.125	5–18	1.018(5)	0.1100(17)	1.2
	0.135	5–18	0.806(4)	0.1149(18)	0.9
	0.145	5–18	0.579(4)	0.1111(21)	0.9
	0.1558	4–11	0.257(8)	0.0821(22)	

$\beta = 6.26 \quad N_S^3 \times N_T = 18^3 \times 48$

κ_1	κ_2	fit range	$a\,M$	$a\,f/Z_A$	χ^2
0.1492	0.09	10–18	1.639(8)	0.0577(26)	0.5
	0.10	10–18	1.433(7)	0.0643(25)	0.4
	0.120	10–23	1.033(5)	0.0784(29)	1.3
	0.135	10–23	0.707(4)	0.0880(25)	1.4
	0.145	6–23	0.461(3)	0.0882(19)	1.3
	0.1492	5–18	0.344(4)	0.0759(33)	1.0
0.1506	0.09	10–18	1.614(11)	0.0517(28)	0.9
	0.10	10–18	1.409(9)	0.0578(26)	0.7
	0.120	10–23	1.003(7)	0.0709(29)	1.4
	0.135	10–23	0.676(4)	0.0799(24)	1.3
	0.145	6–23	0.424(4)	0.0810(21)	1.2
	0.1492	4–18	0.301(4)	0.0672(37)	1.1
	0.1506	4–18	0.254(5)	0.0642(31)	1.0
0.1514	0.09	10–18	1.596(14)	0.0478(29)	0.8
	0.10	10–18	1.391(11)	0.0532(28)	0.7
	0.120	10–23	0.985(9)	0.0662(30)	1.3
	0.135	10–23	0.658(4)	0.0745(26)	1.3
	0.145	6–18	0.407(4)	0.0761(21)	1.1
	0.1492	4–18	0.275(4)	0.0638(39)	1.2
	0.1506	4–17	0.224(5)	0.0596(41)	0.9
	0.1514	4–17	0.189(5)	0.0565(39)	0.7

Table 4:

We give the pseudoscalar decay constant and mass in lattice units extrapolated to κ_u and κ_s, as well as the ratio of the decay constant for a light quark fixed to the strange quark mass to that evaluated at the chiral limit, for all the heavy quarks κ_h considered. The subscript u and s denote quantities evaluated at the chiral limit and at the strange quark mass respectively. The strange quark mass was fixed using the σ scale.

$\beta = 5.74 \quad \kappa_c = 0.1664(5) \quad \kappa_s = 0.1589(3)$

κ_h	$a\, f_u/Z_A$	$a\, M_u$	$a\, f_s/Z_A$	$a\, M_s$	f_s/f_u
0.06	0.1197(102)	2.502(13)	0.1313(74)	2.542(9)	1.097(33)
0.09	0.1629(52)	1.871(13)	0.1726(39)	1.916(9)	1.059(11)
0.125	0.1890(33)	1.205(7)	0.2001(32)	1.253(2)	1.058(10)
0.140	0.1907(38)	0.904(6)	0.2020(29)	0.960(4)	1.059(10)
0.150	0.1829(53)	0.684(5)	0.1947(42)	0.749(4)	1.065(10)

$\beta = 6.00 \quad \kappa_c = 0.1572(4) \quad \kappa_s = 0.1540(3)$

κ_h	$a\, f_u/Z_A$	$a\, M_u$	$a\, f_s/Z_A$	$a\, M_s$	f_s/f_u
0.10	0.0873(17)	1.498(10)	0.0936(16)	1.523(9)	1.073(1)
0.115	0.0983(18)	1.197(7)	0.1048(16)	1.225(4)	1.073(5)
0.125	0.1038(18)	0.995(5)	0.1113(16)	1.026(2)	1.073(6)
0.135	0.1085(19)	0.780(7)	0.1163(16)	0.810(5)	1.072(3)
0.145	0.1032(31)	0.551(2)	0.1123(20)	0.584(4)	1.088(14)

$\beta = 6.26 \quad \kappa_c = 0.1524(6) \quad \kappa_s = 0.1507(4)$

κ_h	$a\, f_u/Z_A$	$a\, M_u$	$a\, f_s/Z_A$	$a\, M_s$	f_s/f_u
0.09	0.0437(32)	1.579(19)	0.0474(30)	1.595(13)	1.086(18)
0.10	0.0486(31)	1.375(14)	0.0529(29)	1.390(11)	1.087(15)
0.120	0.0609(33)	0.965(10)	0.0656(30)	0.983(8)	1.077(13)
0.135	0.0689(29)	0.636(6)	0.0741(25)	0.655(4)	1.074(12)
0.145	0.0711(24)	0.382(4)	0.0757(21)	0.403(3)	1.065(10)
0.1492	0.0580(50)	0.245(4)	0.0628(42)	0.272(3)	1.082(26)

Table 5:

The values of the inverse lattice spacing from the string tension [25], using $\sqrt{\sigma} = 420 MeV$. For comparison we also give the values determined from our f_π and m_ρ data.

β	a_σ^{-1}	$a_{f_\pi}^{-1}$	$a_{m_\rho}^{-1}$
5.74	1.118(9)	1.35(8)	1.41(4)
6.00	1.876(19)	2.36(8)	2.15(10)
6.26	2.775(18)	3.46(37)	2.94(16)

Figure Captions

1. Local masses as defined in eq. 7 for the pseudoscalar meson are plotted versus the time separation t in lattice units. Shown are the data for β =5.74, 6.00 and 6.26 for a light quark mass of about $2m_s$ and a heavy quark mass corresponding to κ_h.

2. Ratio of smeared and local correlators as defined in eq. 8 at $\beta = 6.26$ for different heavy quark masses and a light quark mass of about $2m_s$. Deviations from unity signal contamination of local correlators by excited states. The scale has been set by use of f_π, cf. table 5.

3. Ratio of smeared and local correlators as defined in eq. 8 for $\beta = 6.0$ and 6.26 and a heavy quark mass of about the charm quark mass.

4. f_P vs a in physical units for different meson masses fixed by interpolating between the calculated ones. The lines are linear fits to the data points using only the values where the ratio KMc norm to standard norm is smaller than 1.6. The scale is set by the string tension.

5. $\hat{f}_P$ is shown as a function of $1/M_P$ at β =5.74, 6.00 and 6.26, where the light quark mass is extrapolated to the chiral limit. The set of data points labeled by "KMc" were obtained with the normalization eq. 15 and the dashed lines denote the error band after taking the continuum limit of *these* data. The others denoted by "Standard" are with the relativistic normalization. The static points are taken from ref. [4]. The scale was set by $\sqrt{\sigma}$.

6. $f_P/\sqrt{\sigma}$ is shown vs $L\sqrt{\sigma}$ at $\beta = 5.74$ for different heavy quark masses. The light quark mass was fixed at about $2m_s$.

7. Compilation $f_\pi/\sqrt{\sigma}$ as function of $\sqrt{\sigma}a$. The string tension values are as listed in ref. [4] with linear interpolation in $\ln(a^2\sigma)$. The symbols refer to the results of several groups:
   Filled circle: refs. [23, 6]; Filled square: this work; Filled triangle: ref. [23]; Filled star: refs. [6, 8] and this work; Open circle: ref. [23]; Open square: ref. [22]; Open triangle: this work; Open rhomb: ref. [6]; The star refers to the linearly extrapolated value.

8. $\hat{f}_P$ as function $1/M_P$. The scale is taken from f_π. The lines correspond to the error band described in the text.

Figure 3

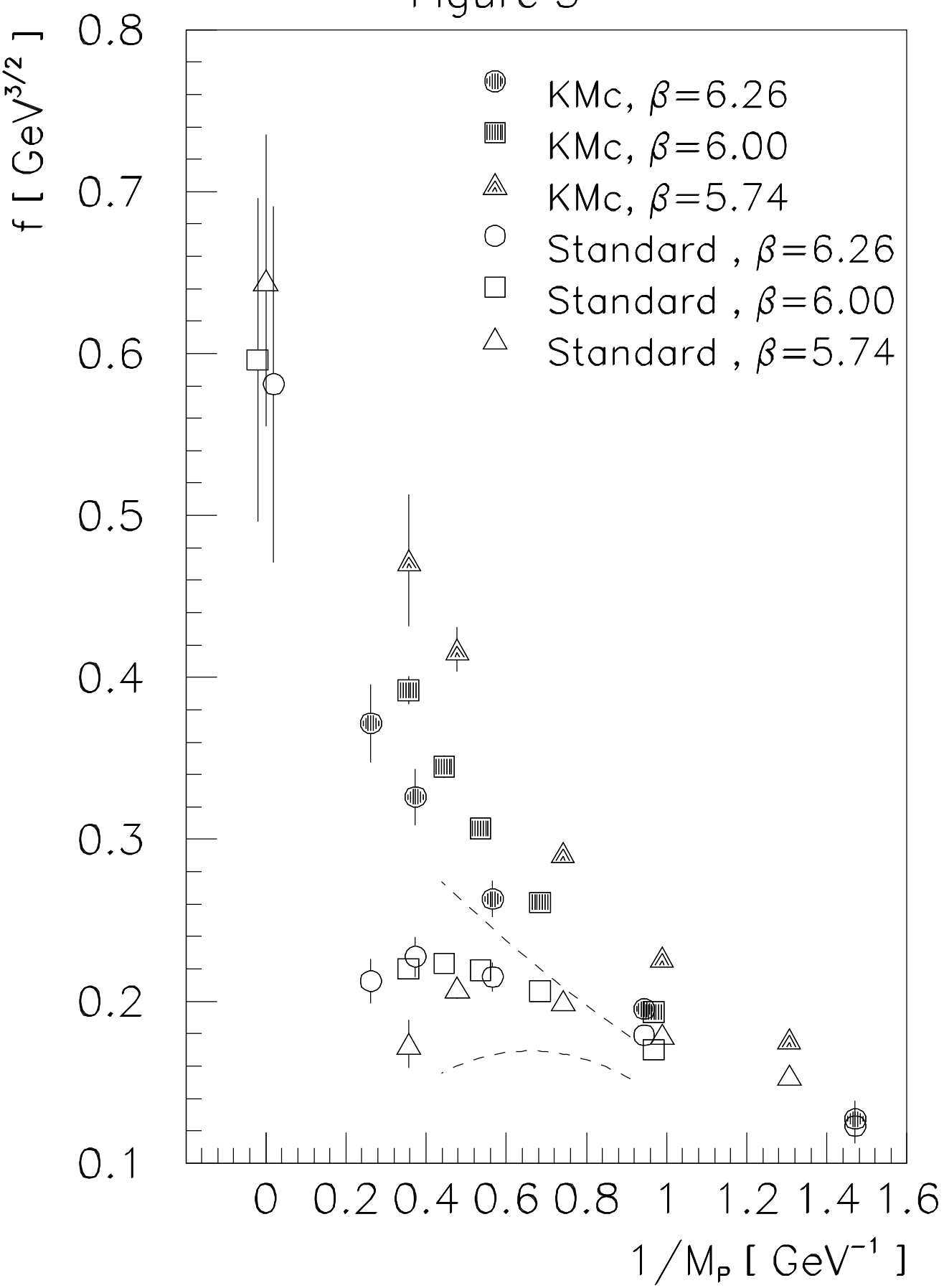
f [GeV^3/2]
0.8
0.7
0.6
0.5
0.4
0.3
0.2
0.1
KMc, β=6.26
KMc, β=6.00
KMc, β=5.74
Standard , β=6.26
Standard , β=6.00
Standard , β=5.74
0
0.2
0.4
0.6
0.8
1
1.2
1.4
1.6
1/M_P [GeV^-1]

Figure 8

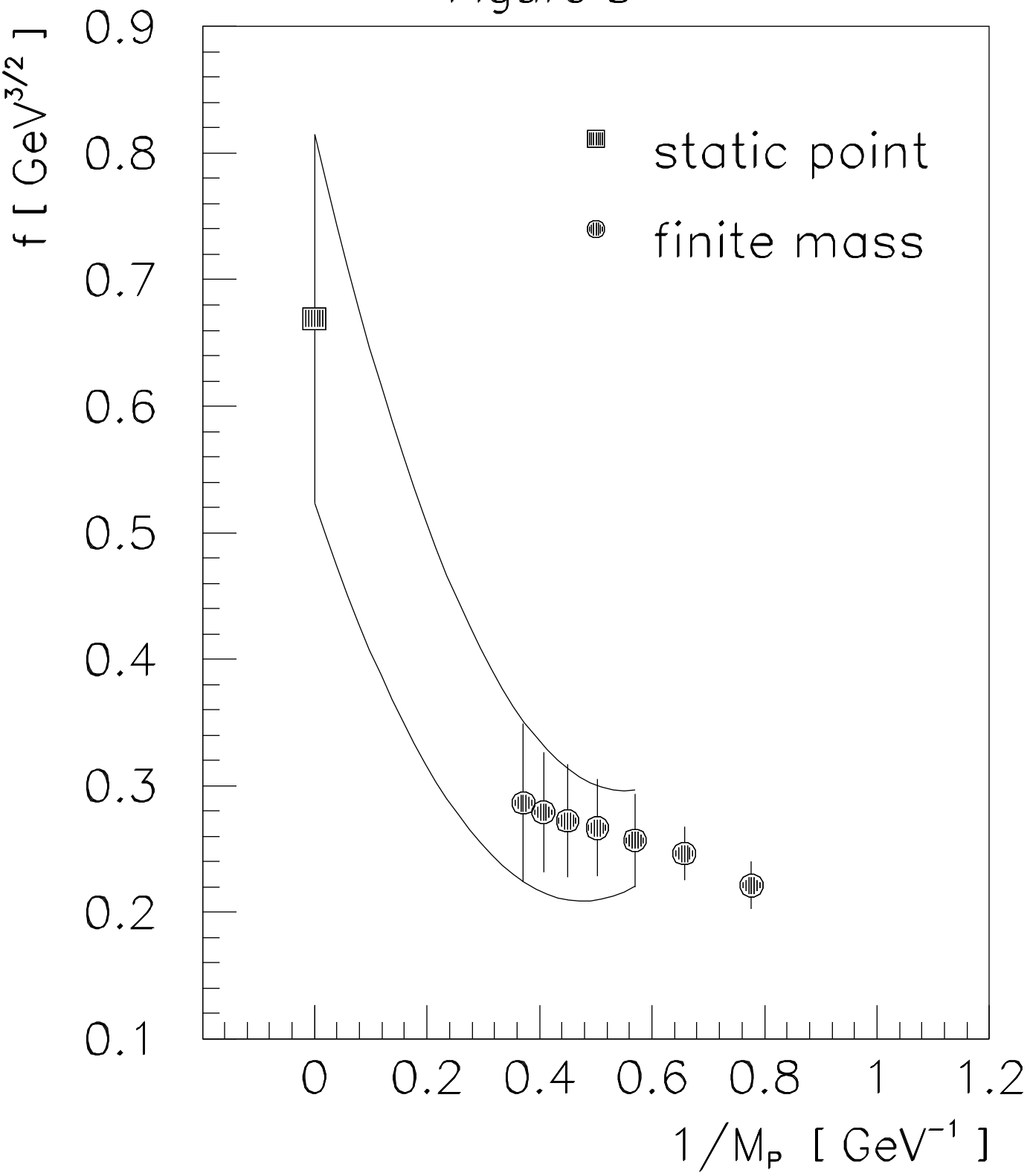
f [GeV^3/2]
0.9
0.8
0.7
0.6
0.5
0.4
0.3
0.2
0.1
static point
finite mass
0
0.2
0.4
0.6
0.8
1
1.2
1/M_P [GeV^-1]

Figure 6

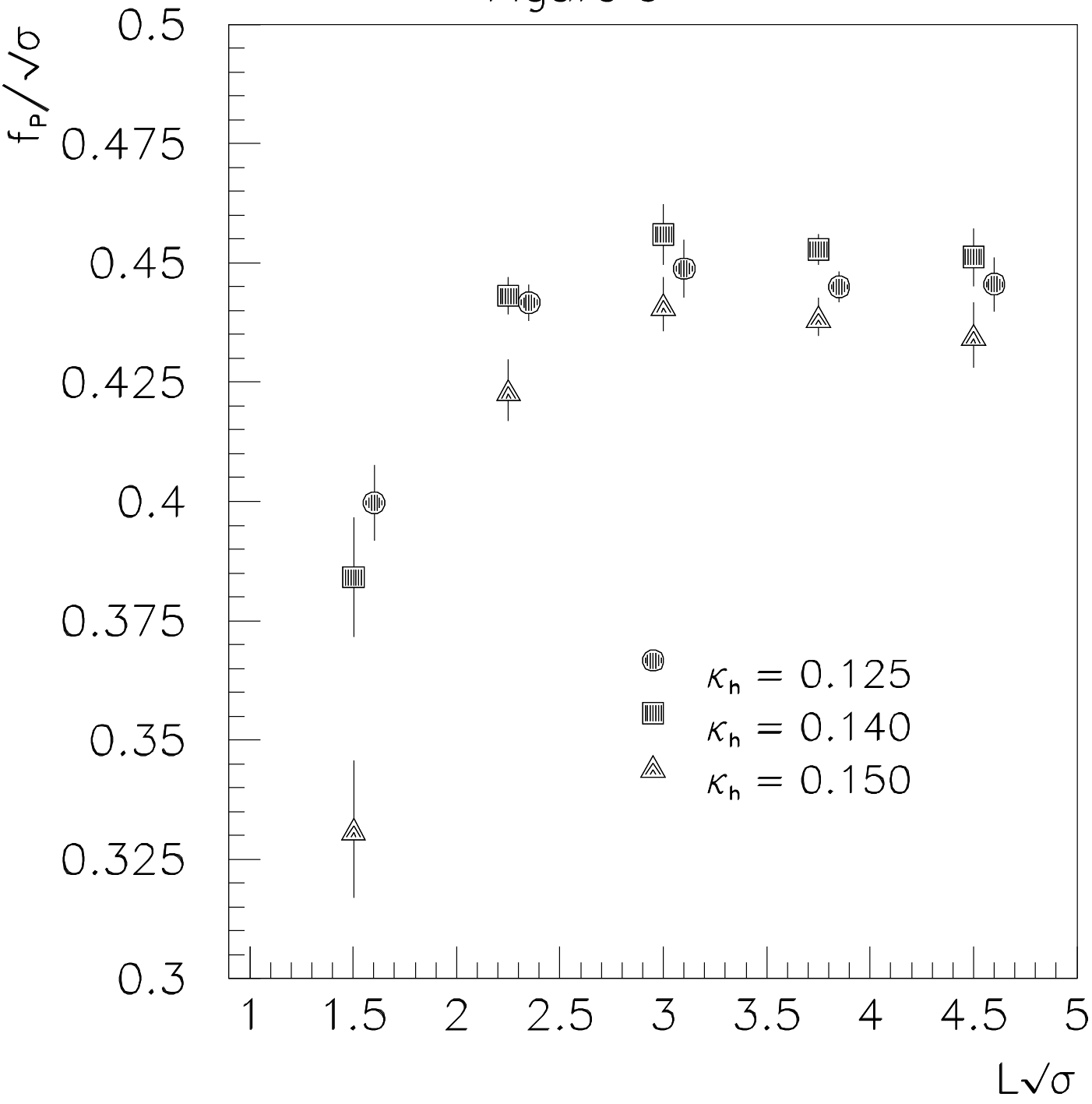
$f_P/\sqrt{\sigma}$
0.5
0.475
0.45
0.425
0.4
0.375
0.35
0.325
0.3
1
1.5
2
2.5
3
3.5
4
4.5
5
$L\sqrt{\sigma}$
$\kappa_h = 0.125$
$\kappa_h = 0.140$
$\kappa_h = 0.150$

Figure 7

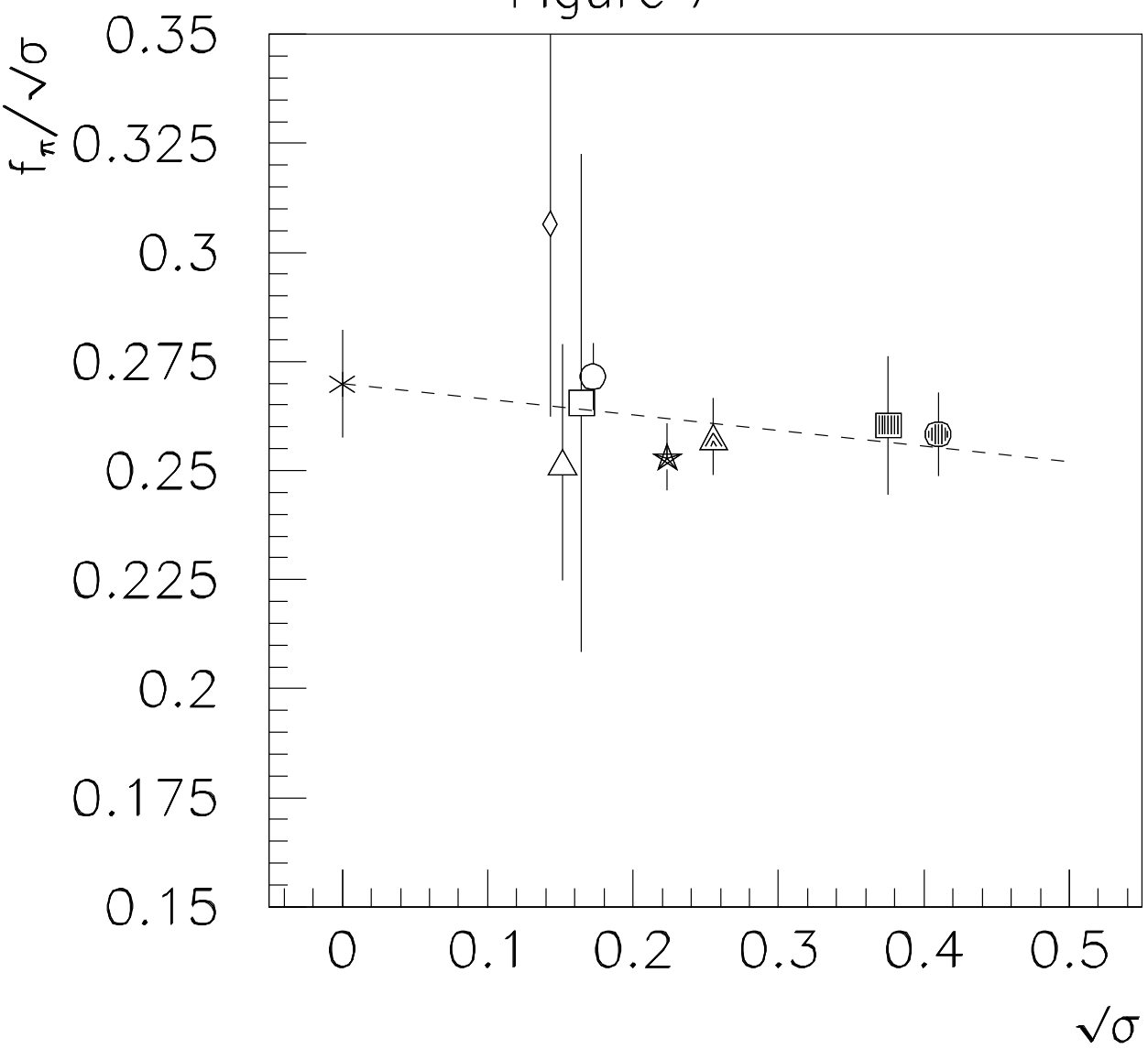
$f_\pi/\sqrt{\sigma}$
0.35
0.325
0.3
0.275
0.25
0.225
0.2
0.175
0.15
0
0.1
0.2
0.3
0.4
0.5
$\sqrt{\sigma}$

Figure 4

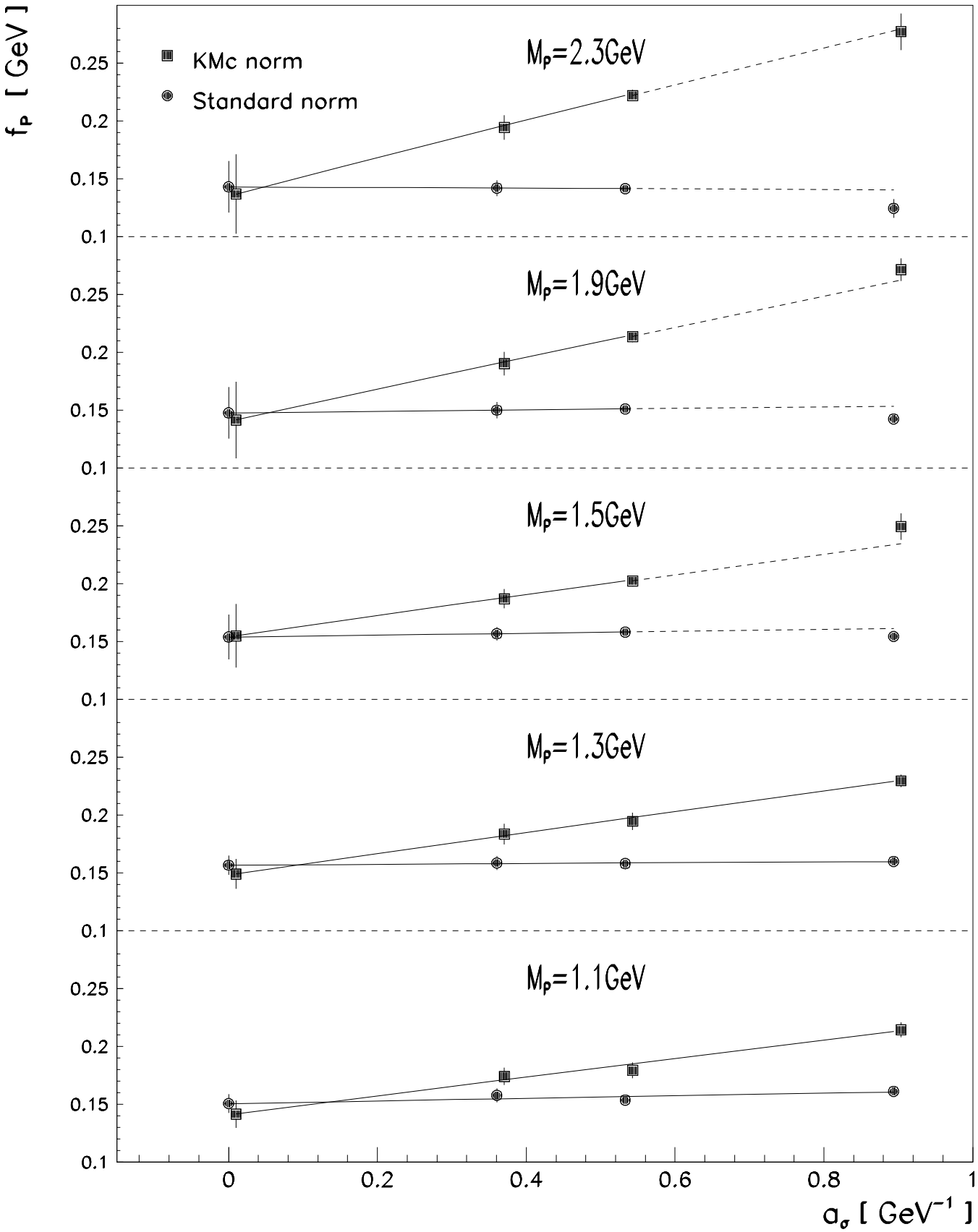
KMc norm
Standard norm
M_ρ=2.3GeV
M_ρ=1.9GeV
M_ρ=1.5GeV
M_ρ=1.3GeV
M_ρ=1.1GeV
f_ρ [GeV]
a_σ [GeV^{-1}]
0.1
0.15
0.2
0.25
0
0.2
0.4
0.6
0.8
1

Figure 1

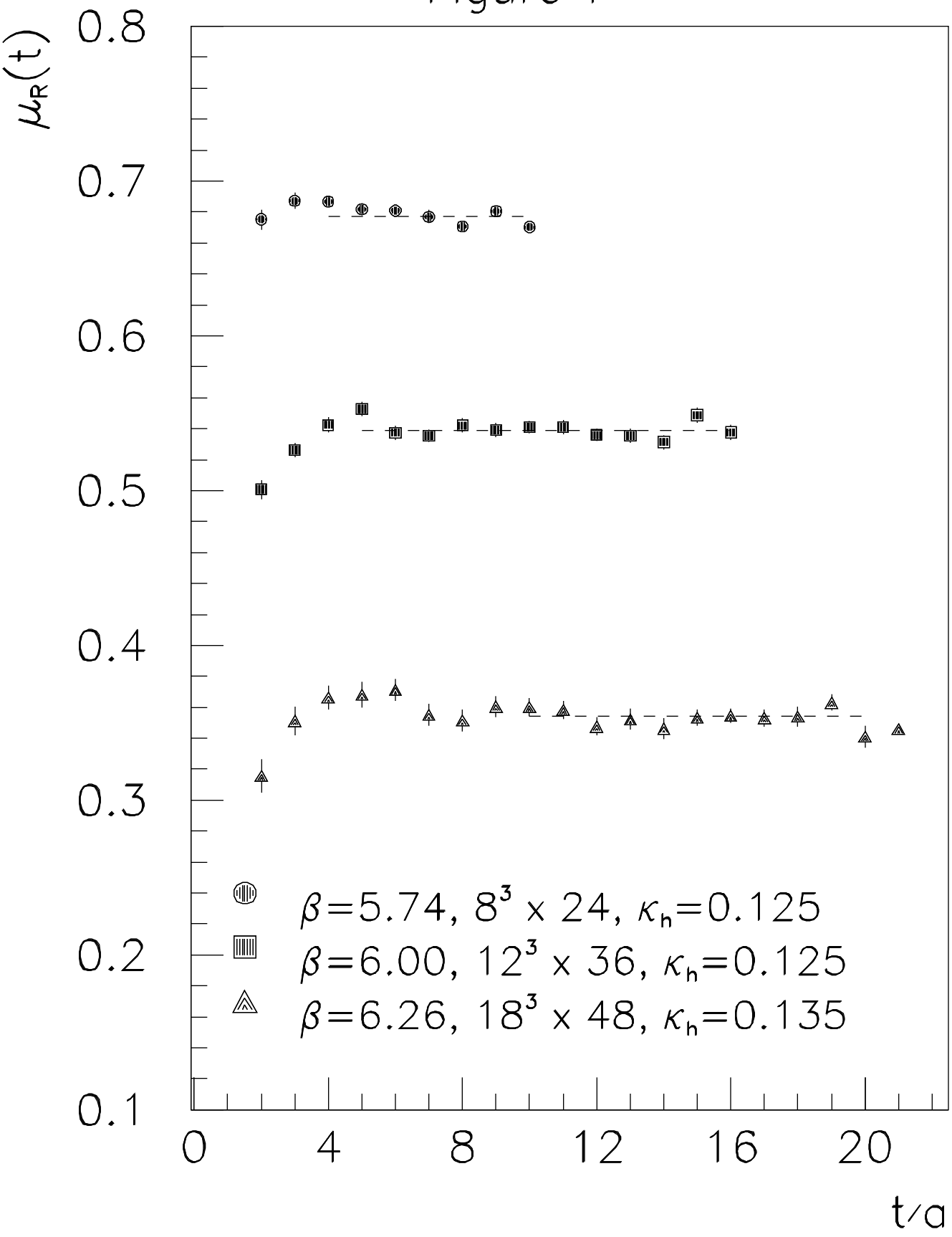
$\mu_R(t)$
0.8
0.7
0.6
0.5
0.4
0.3
0.2
0.1
0
4
8
12
16
20
t/a
β=5.74, 8^3 x 24, κ_h=0.125
β=6.00, 12^3 x 36, κ_h=0.125
β=6.26, 18^3 x 48, κ_h=0.135

Figure 2

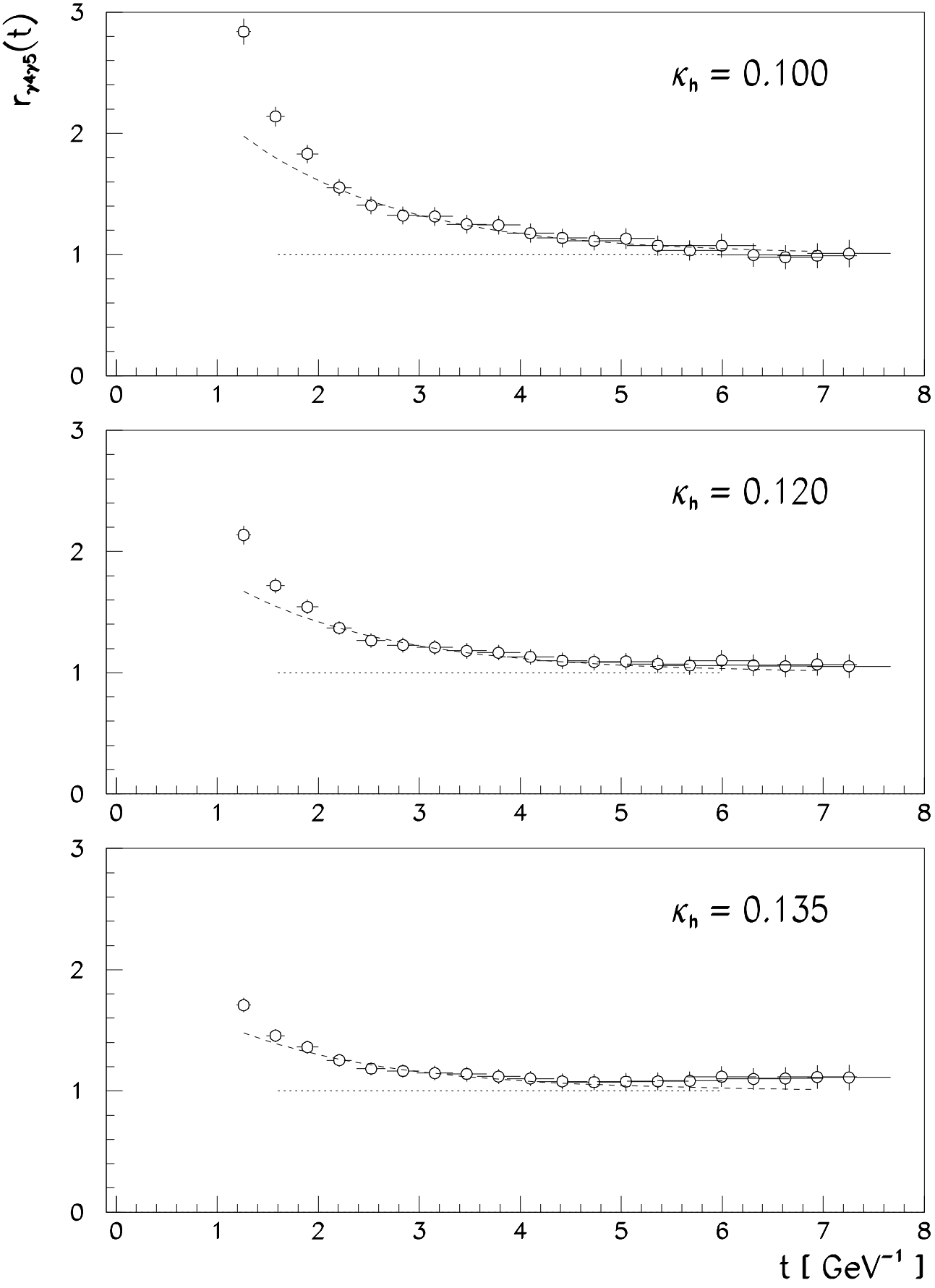

Figure 3